


Spring 4-20-2023

## Analysis and Methodology of Helical and Flexible Homopolymer Monte Carlo Simulations

Nathan Roberts

Follow this and additional works at: <https://digitalcommons.murraystate.edu/honorsthesis>

 Part of the [Biological and Chemical Physics Commons](#), and the [Statistical, Nonlinear, and Soft Matter Physics Commons](#)

---

### Recommended Citation

Roberts, Nathan, "Analysis and Methodology of Helical and Flexible Homopolymer Monte Carlo Simulations" (2023). *Honors College Theses*. 159.  
<https://digitalcommons.murraystate.edu/honorsthesis/159>

This Thesis is brought to you for free and open access by the Student Works at Murray State's Digital Commons. It has been accepted for inclusion in Honors College Theses by an authorized administrator of Murray State's Digital Commons. For more information, please contact [msu.digitalcommons@murraystate.edu](mailto:msu.digitalcommons@murraystate.edu).

Analysis and Methodology of Helical and Flexible  
Homopolymer Monte Carlo Simulations

Nathan Roberts

April 24, 2023

**Submitted in partial fulfillment  
of the requirements  
for the Murray State University Honors Diploma**

# Contents

<b>1</b>	<b>Introduction</b>	<b>1</b>
<b>2</b>	<b>Theoretical Background</b>	<b>3</b>
<b>3</b>	<b>Simulation Methodology</b>	<b>5</b>
3.1	Parallel Tempering Monte Carlo Simulations . . . . .	5
3.2	Hamiltonian Exchange . . . . .	7
3.2.1	FENE potential . . . . .	8
3.2.2	Leonard Jones potential . . . . .	9
3.3	Helical Homopolymer Simulation Methods . . . . .	10
3.3.1	Torsion and bending potentials . . . . .	11
3.4	Flexible Homopolymer Simulation Methods . . . . .	12
<b>4</b>	<b>Data</b>	<b>14</b>
4.1	Equilibration Time . . . . .	14
4.2	Simulation Efficiency . . . . .	16
4.3	Canonical Analysis . . . . .	19
<b>5</b>	<b>Conclusions</b>	<b>21</b>

## Abstract

The purpose of my work is to analyze the results of Monte Carlo simulations of various types of polymers: a helical homopolymer and a flexible homopolymer. Specific applications of Monte Carlo polymer simulations and parallel tempering replica exchanges are presented. Using temporal analysis, I aim to measure the efficiency of each type of simulation as it relates to equilibration time. For the helical homopolymer model, equilibration time is expanded upon to analyze the rate of structure generation and relevant hyper-phase diagram. Stable states for helical homopolymers will use data generated from parallel tempering replica exchange Monte Carlo simulations created by Dr. Matthew Williams. The stable states for flexible polymers will be analyzed and generated using a simulation created by myself. Each simulation begins with a polymer in a random configuration; as time progresses, changes to polymer structure are randomly induced to decrease the energy of each structure until equilibrium is reached. Data collected after equilibrium is reached is used to understand polymer behavior for each model and simulated temperature. Canonical analysis of post-equilibration data yields a specific heat plot for the flexible polymer model and a hyper-phase diagram for the helical polymer model. Analysis of equilibration data shows up to a 95% decrease in equilibration time for the 2D replica exchange scheme over the 1D. Additionally, the incorporation of Hamiltonian exchange into parallel tempering simulations for the helical homopolymer model leads to an average of a seven-fold increase in the rate of unique structure generation. Future research steps involve expanding the application of the 2D replica exchange scheme to differing Monte Carlo simulations as well as the addition of measurable physical and thermodynamic parameters to my simulation.

# 1 Introduction

Generally, a Monte Carlo Parallel Tempering study performs an array of Monte Carlo simulations each at a different temperature. These simulation threads attempt to exchange structures periodically [1]. The structure exchanges provide significantly increased simulation efficiency for low-temperature simulation threads. This paper introduces a parallel tempering technique that simulates a two-dimensional array of simulation threads across temperature and a model parameter of interest. Replica exchanges are attempted between threads of differing temperatures and between threads of differing Hamiltonian [2, 3]. We compare the performance of this two-dimensional parallel tempering approach to that of a set of independent one-dimensional parallel tempering simulations which perform exchanges across temperature alone. The two-dimensional Hamiltonian replica exchanges allow threads to exchange replica configurations across torsional values in addition to temperature values.

The first model, simulated by myself as the original research component of this study, is a coarse-grained flexible homopolymer. Due to time constraints of a single semester for the implementation and analysis of the flexible model [4], replica exchange is performed across only temperature. The coarse-grained helical homopolymer model [5] is used as the test model for the two-dimensional replica exchange algorithm. This is a favorable test model due to its inherent mesoscopic scale, secondary and tertiary structure formation, and structural transitions across both temperature and the torsion parameter [6]. Additionally, this model serves as a useful demonstration because of the biological significance of helical structures [7]. Helical structures and bundles are integral components in a plethora of biological macromolecules such as proteins, nucleic acids, polymers, and composites, among others. The simulation technique presented here is highly flexible and can be easily implemented to study a wide array of systems. The construction of the two-dimensional simulation space makes this technique particularly useful in applications that aim to produce a hyper-phase diagram [8, 9, 10, 11].

The Hamiltonian Exchange which we implement across the second axis of our simulation space is used in other studies with application to Monte Carlo and molecular dynamics simulations. Some examples include explicit water protein folding [12], drug-like molecule bonding [13], harmonic oscillator system and data-guided protein folding [14], MERS-CoV structural dynamics [15] and Amyloid-beta toxicity in Alzheimer’s patients [16]. Other studies have employed various methods for Parallel Tem-

pering optimization such as careful tuning to temperature values to increase simulation speed and efficiency [17, 18] and exchanging replicas between non-neighboring temperature threads [19].

For a parallel tempering simulation, efficiency is often quantified as the average round trip rate for individual replicas [20, 21] or autocorrelation time [22]. To compare the one- and two-dimensional simulations, we adopt two different measures of simulation efficiency: equilibration time and steps per new round-trip traversal. In some instances, simulations proceed with low-temperature threads located in local free-energy minima for a significant number of steps before the energy eventually decreases and remains relatively constant. This can be a real problem for simulations in which the time it would take to find the equilibrium structure is longer than the length of the simulation. We use systems that are small enough to become stable well before the end of the simulation. The time taken to come to equilibrium is measured for each simulation thread. The efficiency of data generation depends on the number of uncorrelated configurations generated. Structures are considered uncorrelated when they have melted and refrozen, meaning they have traversed from a thread at the highest temperature to a thread at the lowest temperature. Since the simulation time in each run varies, the number of Monte Carlo steps per uncorrelated structure is used as the primary measure of efficiency. Faster equilibration times lead to higher acceptance probabilities of exchanges between threads, meaning that more unique polymers can be simulated in a given amount of time. Higher frequencies of replica exchange also yield more unique polymer configurations simulated.

We will demonstrate the use of the data generated by the two-dimensional parallel tempering simulation to produce polymer structures from many different canonical ensembles, analysis of the energy and specific heat for canonical ensembles, and a hyper-phase diagram representing the entire simulation space. Data could be further used to produce a microcanonical analysis or to gain further insight into phase transitions [23, 24]. Microcanonical analysis allows measurement of the density of states and analysis of inflection points.

This paper is organized as follows. In the Theoretical Background section, we introduce the application and background of one-dimensional and two-dimensional parallel tempering algorithms for representing simulated helical and flexible homopolymers in addition to the description of the Monte Carlo method of sampling the virtual structural environment. The Simulation Methodology section

details the methodology of both the flexible and helical homopolymers. Data details analysis of data obtained from each type of polymer simulation with a focus on comparison and discussion between one-dimensional and two-dimensional parallel tempering or replica exchange algorithms and their correlation to simulation efficiency. The paper is concluded by the summary and future research steps in Conclusions.

## 2 Theoretical Background

Polymers, simply defined as a collection of bonded monomers, make up materials ranging from polyester to nucleic acids found within all life. For this reason, polymer chemistry and subsequently its molecular properties are difficult and tedious to study in a laboratory environment. Simulations such as Monte Carlo and Molecular Dynamics allow efficient study of thermodynamic and structural properties for simulated models. Fine-grained polymer models quantify energy between each individual atom within a molecule of a polymer chain, while coarse-grained models treat repeated units of the chain as individual monomers. Therefore, to simulate real systems, a measure of energy must be calculated and used to quantify configurations in thermodynamic equilibrium.

Polymer energy, when modeled in simulations, are characterized by a Hamiltonian. The Hamiltonian quantifies each force that acts on a polymer and assigns a corresponding energy value to it. In this work, we consider two distinct models: a flexible homopolymer and a helical homopolymer. Both the flexible and helical homopolymer models chosen contain Hamiltonians for known atomic forces. These include the Lennard-Jones potential, an effective potential representing the Van der Waals and Pauli Exclusion Principle, and a FENE potential which treats monomers as point masses and bonds as springs. The helical polymer model contains additional potentials in both the torsion and bending energy which impart a helical order to the structures. The bending potential is associated with bond angles, while the torsion potential is associated with the dihedral angles formed by each series of three bonds. For the helical study, the data presented correspond to polymer chains of length  $N = 30$ . This system provides a sample model to accurately compare simulation methods.

Computational physics simulations contain many other useful parameters that correspond to features in physical systems. Some of these include the excluded volume, the LJ Fraction, three-body

interaction coefficient, and the aspect ratio of monomers. Due to the coarse-grained model chosen for these studies, the aspect ratio  $b/d$  holds no relevance, as the size of monomers does not vary across the length of the polymer chain. The excluded volume  $v$  and three-body interaction coefficient  $w$  are more applicable in simulations of polymer reactions with given substrates. Future studies of reactions of the flexible and helical homopolymer models would benefit from tracking parameters  $v$  and  $w$ . In addition, the next steps to further the research towards the quantification of a real system rather than theoretical would involve the inclusion of thermodynamic properties of each monomer to simulate known configurations of polymer chains. One common example of a polymer is polystyrene, a hydrocarbon plastic found in styrofoam, food packaging, and lab equipment. For a coarse-grained simulation of polystyrene, for example, each monomer of a  $N$ -length polystyrene chain would contain  $CH_2$  molecules with branching side-chain phenyl ( $CH$ ) groups. Properties of the elements Hydrogen and Carbon, such as atomic radius, atomic weight, and electronegativity, among others, would need to be incorporated into the simulation and the Hamiltonian of the system.

The benefit of simulating generalized models lies in their simplicity and the ability to study the general behaviors of models. Modeling the interaction of two specific materials, such as polystyrene and a substrate designed to dissolve it, yields results that are only applicable to that specific reaction. Conversely, a study of the general behavior of polymers using known physical forces yields insight into how a polymer would react in a given environment regardless of its material properties. In addition, simpler, coarse-grained models require less computation time to complete, meaning that results can be analyzed and interpreted more quickly. For more comprehensive research on other models, other parameters such as the excluded volume and overlap probability of monomers could be useful [25]. Since this research evaluates the effectiveness of a simulation technique, interpreting and evaluating the simulation data is more essential than the specific application. The two-dimensional parallel tempering replica exchange can be applied to any Monte Carlo simulation and the torsion value  $S_\tau$  can be substituted for any useful parameter.



### 3 Simulation Methodology

#### 3.1 Parallel Tempering Monte Carlo Simulations

The helical homopolymer simulation in this paper consists of an array of simulation threads with each thread generating a canonical ensemble at temperature  $T$  and obeying Hamiltonian  $H$ . This two-dimensional array of threads can be visualized as a grid shown in Fig. 1. The flexible model threads in this study vary solely across temperature. Threads independently proceed with Monte Carlo updates. Each update changes the energy of the structure by  $\Delta E$ . Updates are accepted with probability  $P_{\text{acc}} = e^{-\beta\Delta E}$ , where  $\beta = 1/T$ .

Simulations denoted as "displacement only" use only single monomer displacement updates. Simulation efficiency can be moderately improved by the addition of multiple global update types. These simulation runs are denoted "displacement + global" and include simultaneous displacement of a collection of monomers, change of a single bend angle by rotation of one side of the polymer around an axis perpendicular to neighboring bonds, and changing of a single dihedral angle by rotation of one side of the polymer around an axis defined by one bond.



parallel tempering in Python.

Two different replica-exchange Monte Carlo techniques are utilized for the helical polymer model. In the temperature-only approach, which will be referenced as one-dimensional, simulation threads attempt replica exchange with an adjacent higher temperature thread and then with an adjacent lower temperature thread. This sequence of replica exchanges is repeated at each Monte Carlo step. In the flexible polymer model, only one-dimensional replica exchanges are attempted. In Fig. 1, these are depicted as black arrows.

### 3.2 Hamiltonian Exchange

The second type of replica exchange in this study involves exchanging structures across threads at neighboring Hamiltonians. The Hamiltonian for each replica, described in the theoretical background section, is then used as a parameter to perform exchanges. Attempting replica exchanges is a form of Monte Carlo time steps [28] utilized to traverse a two-dimensional space defined by temperature and a suitable model parameter. Replica exchange serves to prevent threads from conforming to structures "stuck" in local minima of the free energy landscape of a polymer. At each fixed interval of a Monte Carlo time step, adjacent threads attempt to exchange with one another to "pass" structures to neighboring threads. Along the free energy landscape of the polymer model, there exists an ideal global minimum energy that a polymer can reach. Since the nature of Monte Carlo simulations is random moves, sampling more of the free energy landscape of the polymer model serves to better represent structures of a particular canonical ensemble. Final thread structures are heavily influenced by the temperature of the system which corresponds to the random kinetic energy of the polymer and its environment. The total energy of a replica is represented in a Hamiltonian  $H$  shown in equation 1.

$$\begin{aligned}
H(\mathbf{X}) = & S_{\text{LJ}} \sum_{i>j+1} v_{\text{LJ}}(r_{ij}) + S_{\text{FENE}} \sum_i v_{\text{FENE}}(r_{i\ i+1}) \\
& + S_{\tau} \sum_l v_{\text{tor}}(\tau_l) + S_{\theta} \sum_k v_{\text{bend}}(\theta_k)
\end{aligned} \tag{1}$$

To accomplish Hamiltonian exchanges across neighboring replicas (directly adjacent in either temperature or torsion potential  $S_{\tau}$ , we employ the Metropolis algorithm, first employed by Nicholas Metropolis in his work on nuclear reactors [29]. Initially, a uniformly distributed random number

between 0 and 1  $P_{rand}$  is generated and compared to the acceptance probability  $P_{acc}$  given in equation 2.

$$P_{acc} = \frac{e^{\beta_i H_i(X_i)} e^{\beta_j H_j(X_j)}}{e^{\beta_i H_i(X_j)} e^{\beta_j H_j(X_i)}}. \quad (2)$$

In the case of a temperature exchange,  $H_i = H_j \equiv H$  and Equation 2 becomes

$$P_{acc,T} = e^{(\beta_i - \beta_j)(H(X_i) - H(X_j))}. \quad (3)$$

For the Hamiltonian exchange,  $\beta_i = \beta_j \equiv \beta$  and Equation 2 becomes

$$P_{acc,H} = e^{\beta(H_i(X_i) + H_j(X_j) - H_i(X_j) - H_j(X_i))}. \quad (4)$$

If  $P_{rand}$  is greater than  $P_{acc}$  then a Hamiltonian exchange is made. This occurs once every 500 moves as a Monte Carlo time step. Changes in  $H$  within the flexible polymer model represent a change in the temperature  $T$ . In the helical polymer model, changes in  $H$  represent a change in the torsion energy scale factor  $S_\tau$  in addition to the aforementioned temperature exchange. Herein lies the novelty of Dr. Williams' research: the ability to perform replica Hamiltonian exchanges across both temperature and torsion values. Hamiltonian exchanges are represented by gray arrows in Fig. 1. In this way, replicas perform a two-dimensional random walk in the  $S_\tau$  -  $T$  space. While two-dimensional Hamiltonian exchanges have been applied to other types of simulations such as Molecular Dynamics, the nature of the Monte Carlo simulation creates a significant difference in the performance of the Hamiltonian Exchange. The two-dimensional Hamiltonian exchange can be expanded to any suitable model parameter, not just the torsion energy scaling factor  $S_\tau$ .

### 3.2.1 FENE potential

Bonded monomers interact according to the finitely extensible nonlinear elastic (FENE) potential [30, 31]. The FENE potential, given in Equation 5, depends solely on the distance between the two bonded monomers,  $r$ . A graph of this function is shown in Fig. 2. The FENE potential quantifies the mechanical energy of a given polymer. It treats each monomer as a point mass and each bond as an ideal spring. A minimum bond energy is achieved when  $r = r_0 \equiv 1$  and the maximum deviation from this value is  $R \equiv 3/7$ . Any move which separates two bonded monomers by more than  $r + R$  or brings them closer than  $r - R$  is immediately rejected. This is due to equation 5 and its inherent logarithmic

quantity. Since the definition of a logarithmic function is a positive quantity to an exponential degree, any negative quantities do not lie within the domain of the function. For equation 5, this corresponds to any value with a magnitude greater than  $r + R$ .

### 3.2.2 Leonard Jones potential

Each monomer also interacts with all other monomers according to the Lennard-Jones (LJ) potential. A graph of this potential is shown in Fig. 2. The Lennard-Jones potential has two forces: a short-range repulsive force due to overlapping electron orbitals and an attractive Van Der Waals force [32]. This relationship is given in equation 6. This function reaches a minimum when monomer separation approaches a distance  $r_0$ . We induce this by utilizing a parameter  $\sigma \equiv 2^{-1/6}r_0$  equal to the theoretical minimum value of  $v_{LJ}$ . Fig. 3 shows the ideal characteristic function of the Lennard-Jones potential. In order to avoid discontinuities in the Hamiltonian energy calculation, we shift the Lennard-Jones potential by a constant value  $v_c = 4[(\sigma/r_c)^{12} - (\sigma/r_c)^6]$ .

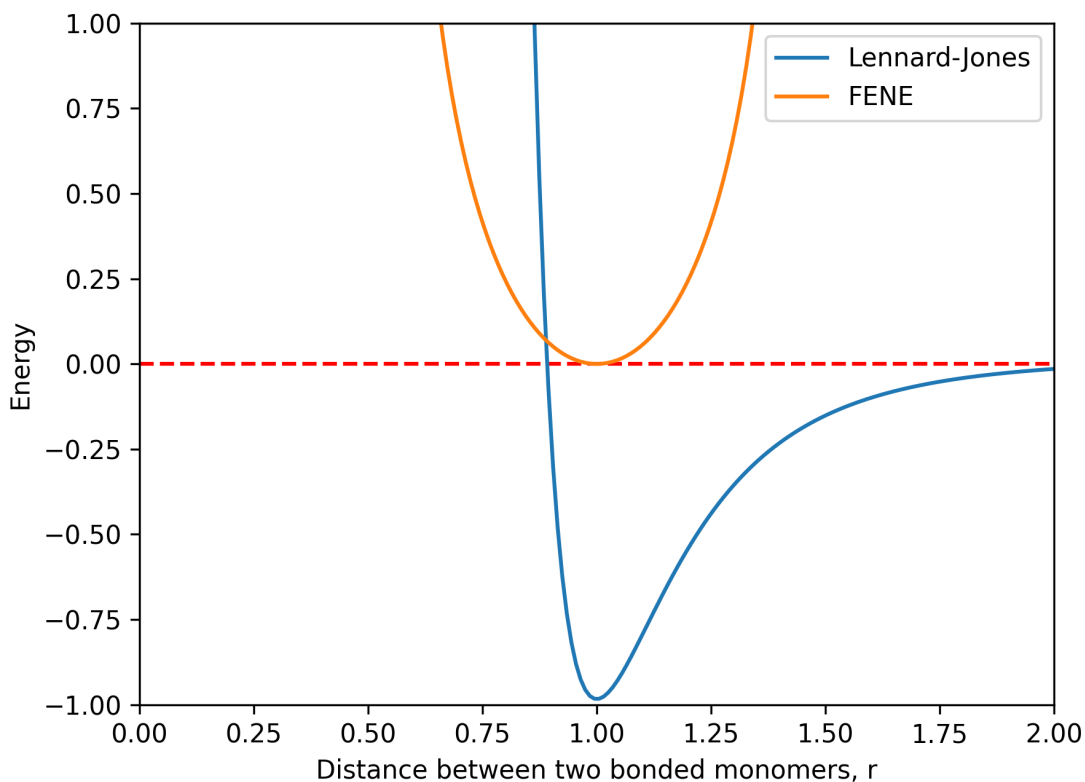


Figure 2: A visual representation of the Lennard-Jones and FENE potential values used in both the flexible and helical homopolymer models.

### 3.3 Helical Homopolymer Simulation Methods

A portion of this study employs the use of a coarse-grained homopolymer model which is designed to generate helical secondary structures. In past work, this model has been shown to also exhibit tertiary structures consisting of two- and three-helix bundles. Tertiary structure formation depends on the details of the model parameters. The energy of a polymer chain with  $N$  monomers includes four potentials: a bonded interaction between neighboring monomers along the polymer chain, a non-bonded interaction between monomers in physical proximity, a bending potential, and a torsion potential. In this study, we present data for polymer chains of length  $N = 30$ . This system provides a sample model to accurately compare simulation methods.

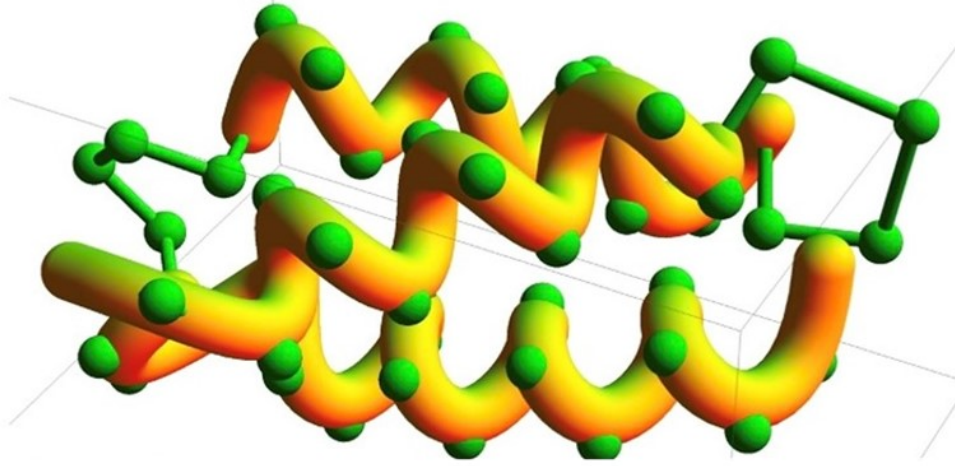


Figure 3: A visual representation of the helical homopolymer model generated by Matthew Williams and Michael Bachmann [5].

### 3.3.1 Torsion and bending potentials

The helical order is imparted using bending and torsion potentials given by Equations 7 and 8, respectively. The bending potential depends on the bond angle of successive bonds,  $\theta$ . There is a potential minimum for  $\theta = \theta_0 \equiv 1.742$ . The torsion potential depends on the successive dihedral angles,  $\tau$ . There is a potential energy minimum when  $\tau = \tau_0 \equiv 0.873$ .

$$v_{\text{FENE}}(r) = \log\{1 - [(r - r_0)/R]^2\} \quad (5)$$

$$v_{\text{LJ}}(r) = 4[(\sigma/r)^{12} - (\sigma/r)^6] - v_c \quad (6)$$

$$v_{\text{bend}}(\theta) = 1 - \cos(\theta - \theta_0) \quad (7)$$

$$v_{\text{tor}}(\tau) = 1 - \cos(\tau - \tau_0) \quad (8)$$

The total potential energy of a particular polymer configuration  $\mathbf{X}$  can be calculated using the Hamiltonian given in Equation 1. The Hamiltonian consists of all four potentials applied across the entire polymer with each potential multiplied by an energy scale. We use the standard values of  $S_{\text{FENE}} = -(98/5)r_0^2 R^2/2$  and  $S_{\text{LJ}} = 1$  for the FENE and LJ energy scales. A bending energy scale of  $S_\theta = 200$  is used for all simulation threads. In an effort to analyze an array of systems with different tertiary structure formations, values between 5 and 14 are used for  $S_\tau$ .

### 3.4 Flexible Homopolymer Simulation Methods

To gain a broader understanding of the methodology behind the helical homopolymer simulation previously analyzed by the research team, I was tasked with creating another well-studied model of polymer simulation: the 13-monomer flexible homopolymer. The flexible polymer model adheres to only the Lennard-Jones and FENE potentials. Consequently, it forms entirely different structures than the helical homopolymer model and exhibits unique thermodynamic properties. The original component of my research lies in the language the simulation is built in. While Dr. Williams' helical homopolymer simulations were programmed in the language of C++, my simulation was programmed entirely within Python, an open-source and easily accessible language. This simulation was developed and improved upon over the course of the Spring 2023 semester. In total, the simulation, which consists of three different programs, is about 600 lines of code and took around 6 weeks to complete.

The flexible homopolymer simulation is a simplified version of the helical homopolymer model. This was chosen due to the time constraint of a single semester for the development and implementation of the simulation. The flexible model adheres to the FENE and Lennard-Jones potentials but is not constrained by the bending and torsion angles. Therefore, the flexible polymer model Hamiltonian consists of the FENE and LJ potentials given in equations 5 & 6. The total energy is represented as a Hamiltonian  $H_f$  shown in equation 9.

$$H_f(\mathbf{X}) = S_{\text{LJ}} \sum_{i>j+1} v_{\text{LJ}}(r_{ij}) + S_{\text{FENE}} \sum_i v_{\text{FENE}}(r_{i,i+1}) \quad (9)$$

Since the incorporation of torsion and bending potentials cause a polymer to conform to helical shapes, the lack thereof in the flexible model forms an entirely different set of structures. With a low-temperature 13-monomer chain, the predicted lowest energy state is an icosahedron, a platonic solid containing 30 edges, 20 faces, and 12 vertices. In this 13-monomer configuration, twelve monomers form the vertices, with the thirteenth residing in the shape's center. This shape exhibits platonic symmetry with each of its 20 triangular faces. Fig. 4 was plotted in Mathematica, with green spheres representing monomer coordinates output by my simulation. The monomers are treated as point masses mathematically but are modeled with a finite size to show the structure of the polymer.



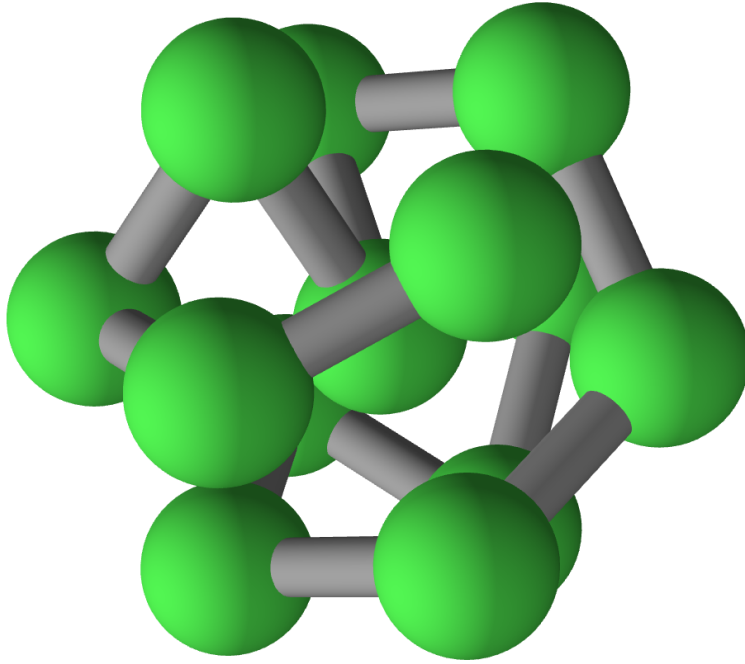


Figure 4: Depiction of final polymer structure at  $T = 0.2$  generated by the developed flexible polymer simulation. Polymer structures from my simulation were plotted using Mathematica code developed by Dr. Williams.

At higher temperatures, the flexible model forms a globule shape, as shown below in Figure 5. This structure's monomers are also point masses mathematically but are plotted with a finite size to visually represent the polymer structure. This structure lacks the order that structures conform to in lower temperatures and is considered a "liquid" state. Using canonical analysis, it is possible to identify where these structure transitions occur across simulated temperature values.

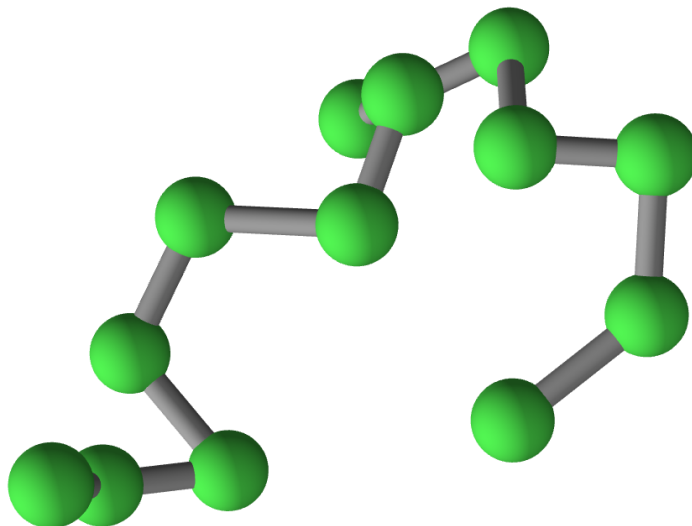


Figure 5: Depiction of final polymer structure at  $T = 0.7613$  generated by the developed flexible polymer simulation. Polymer structures were plotted using Mathematica code developed by Dr. Williams.

## 4 Data

### 4.1 Equilibration Time

One of the first tasks given by my research mentor in the analysis of 2-D parallel tempering replica exchange simulations was plotting the energy values of the helical polymer over time. This was done in order to construct the hyper-phase diagram of the helical homopolymer model, which will be discussed later in this section. Hyper-phase diagrams, which graphically illustrate the thermodynamic behavior of polymer models across an array of temperature values, must use data that is considered to be at thermodynamic equilibrium.

The determination of thermodynamic equilibrium, however, can be characterized by multiple data analysis algorithms. The research team evaluated multiple algorithms for equilibration determination. The first characterized a data time series as "in thermodynamic equilibrium" when all values of a 400-point moving average oscillated within one standard deviation of the last 10% of the energy time series. This algorithm correctly identified thermodynamic equilibrium for most replicas but failed in cases of a replica "jumping" from one energy value to another throughout the time series. An example of this is shown below in Figure 6.

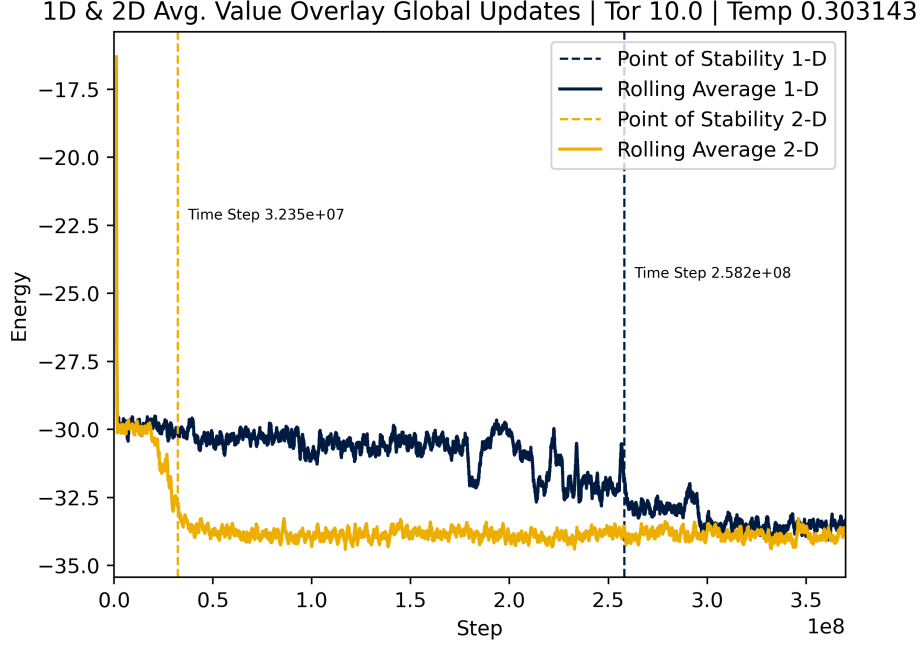


Figure 6: Energy of the helical homopolymer model plotted against Monte Carlo time steps. Equilibration time was calculated using the first equilibration algorithm. This specific thread corresponds to a torsion parameter of 10 and a temperature value of 0.303.

The algorithm currently in use for determining thermodynamic equilibrium involves first identifying the global minimum of the data time series. Because the goal of the model is to reach a state of thermodynamic equilibrium by the end of the simulation, the global minimum energy value is assumed to be at or near a stable polymer configuration. Once the global minimum,  $E_g$ , is found, the average of all time series energies after the global minimum is computed. This is referred to as  $\bar{E}$ . The value  $t_{\text{eq}}$  is considered to be the point at which the rolling average of the energy value first crosses below  $\bar{E}$ . For each value of  $S_\tau$  considered in the simulation, we find the thread with the maximum  $t_{\text{eq}}$ . This maximum,  $t_{\text{max}}$ , is calculated for each value of  $S_\tau$ . The maximum time to equilibrium is given for the 1D and the 2D simulation in Table 1.

In this specific model, simulations containing exclusively 1D parallel tempering exchange schemes exhibit lengthy equilibration times. Fig. 7 shows the energy time series and equilibration times  $t_{\text{eq}}$  for both the 1D and 2D exchange scheme within the thread at  $T = 0.2$  and  $S_\tau = 11$ . For this example, we see a sharp decrease in equilibration time for the 2D simulation.

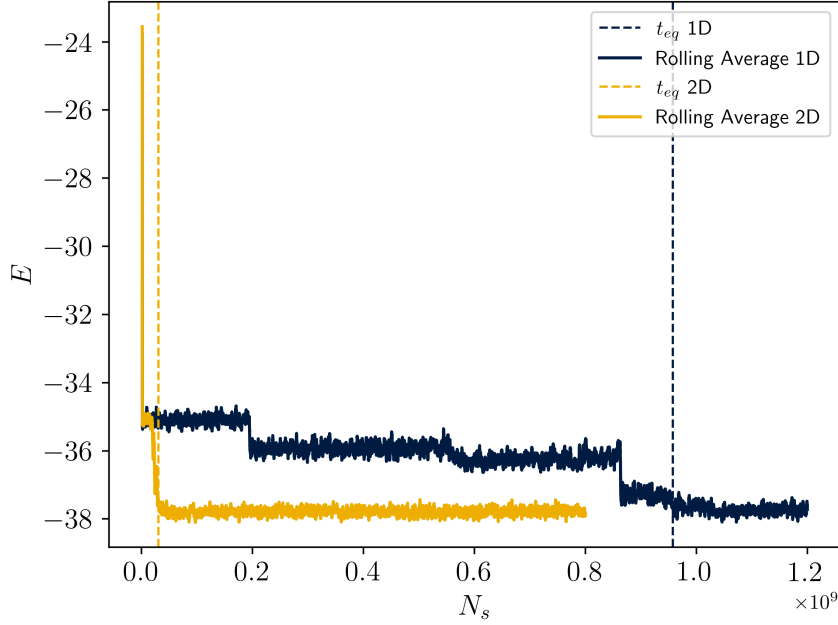


Figure 7: Energy of a one- and two-dimensional parallel tempering simulation vs. Monte Carlo time step. This data comes from the displacement-only run. For this graph,  $S_\tau = 11$  and  $T = 0.2$ . Solid lines represent rolling averages with a window size of 250 time-series measurements.  $t_{eq}$  is analytically determined by the stability algorithm and plotted as a vertical dashed line.

The torsion strength value  $S_\tau$  ranges from 5 to 14 in this simulation, with low  $S_\tau$  threads favoring multi-helix bundles and high  $S_\tau$  threads favoring single-helix bundles. At intermediate  $S_\tau$  values (9-11), random coil-like structures begin to appear due to the inability of the simulation to find a structure with lower energy in both single-helix and multi-helix bundles. This leads to longer equilibration times which causes the likelihood of replica exchange between neighboring replicas to decrease. Therefore, a given structure would take longer to walk the two-dimensional space from a "melted" state to a low-temperature thread.

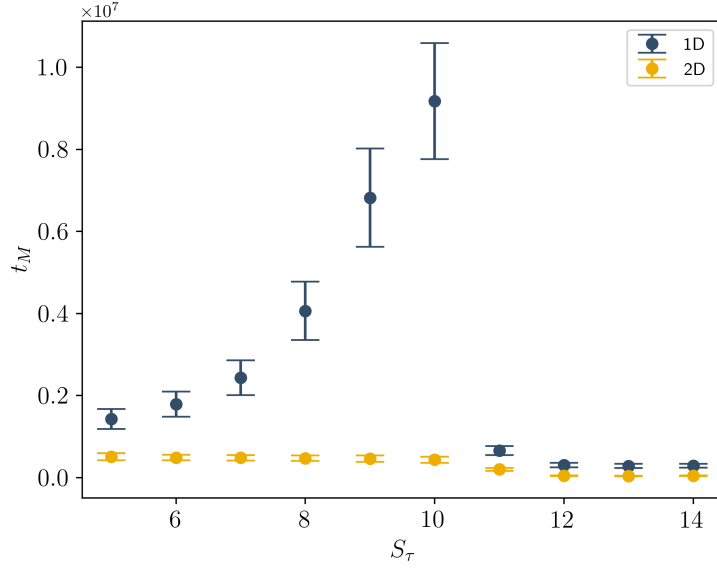
## 4.2 Simulation Efficiency

Simulation efficiency can be quantified in multiple fashions for simulations with a sizable number of parameters. In other notable examples, efficiencies were related to the average round-trip rate for individual replicas. In this study, we characterize efficiency as a function of the average number of

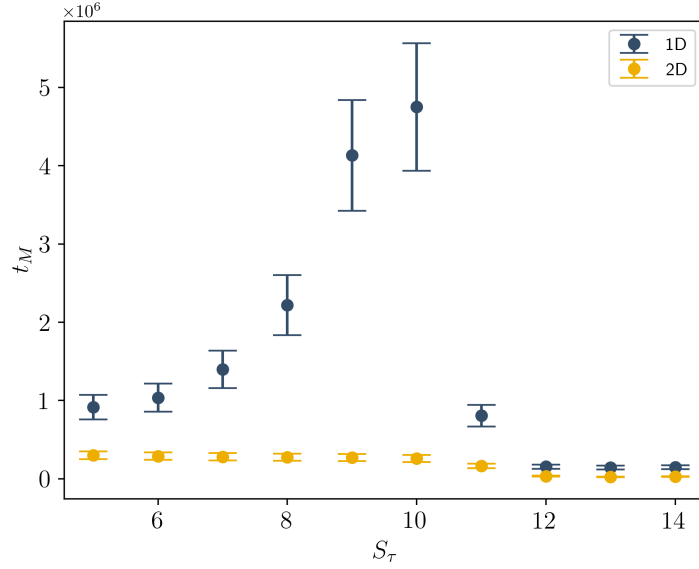
Table 1: Equilibration time for the 1D and the 2D displacement only parallel tempering simulation.

$S_\tau$	$t_{max_{1D}}$	$t_{max_{2D}}$
	$\times 10^6$	$\times 10^6$
5	25.3	49.8
6	49.2	48.4
7	35.4	45.3
8	109	54.0
9	150	47.8
10	296	50.6
11	1020	49.4
12	559	39.7
13	1.88	1.74
14	3.42	4.64

Monte Carlo steps per new structure generated for each replica,  $t_M$ . At each torsion value, low-temperature threads identify each new structure generated and assign a unique identifier to each one and a time stamp. As Monte Carlo time steps pass and replica exchanges occur between neighboring threads, a replica will "walk" through the two-dimensional space. High-temperature threads then identify structures as "melted". If a low-temperature thread receives a "melted" structure, the traverse time for that replica is logged. This process is done at each torsion value  $S_\tau$  as shown in 8 for both the one-dimensional and two-dimensional replica exchange schemes.  $t_M$  represents the average number of time steps per new and unique generated structure.



(a) Displacement-only



(b) Displacement + Global

Figure 8: Average number of time steps per unique configuration measured against the torsion value of the thread for 1-D and 2-D parallel tempering Hamiltonian exchanges for helical homopolymers. The solid points represent the average number of time steps between the appearance of a unique replica structure after energy equilibration at corresponding torsion values shown with sampling errors. (a) corresponds to displacement-only simulations and (b) represents simulations with displacement + global updates.

As shown in Figure 8, the two-dimensional replica exchange scheme decreases  $t_M$  for all torsion strength values between 5 and 14 with the largest decreases occurring at intermediate torsion values. Across all torsion values, the implementation of a two-dimensional exchange scheme leads to a seven-fold increase in the rate of generated structures in the helical model. This value holds true for both the displacement-only and displacement + global update schemes.

### 4.3 Canonical Analysis

In addition to data collected on the effectiveness of simulation techniques, the prevalent structures of polymer models are useful in visualizing free energy. To determine structural transitions across temperature values, a specific heat vs. temperature plot is used. Peaks in the specific heat of the polymer ( $dE/dT$ ) correspond to transitions in structure types. Analyzing peaks in the specific heat at each torsion value allow a two-dimensional representation of the range of polymer configurations. For the flexible polymer model, the specific heat plot can be found below in Figure 9. The Figure shows a clear maximum occurring at  $T \approx .35$ , indicating a transition from an icosahedral structure to a globular structure.

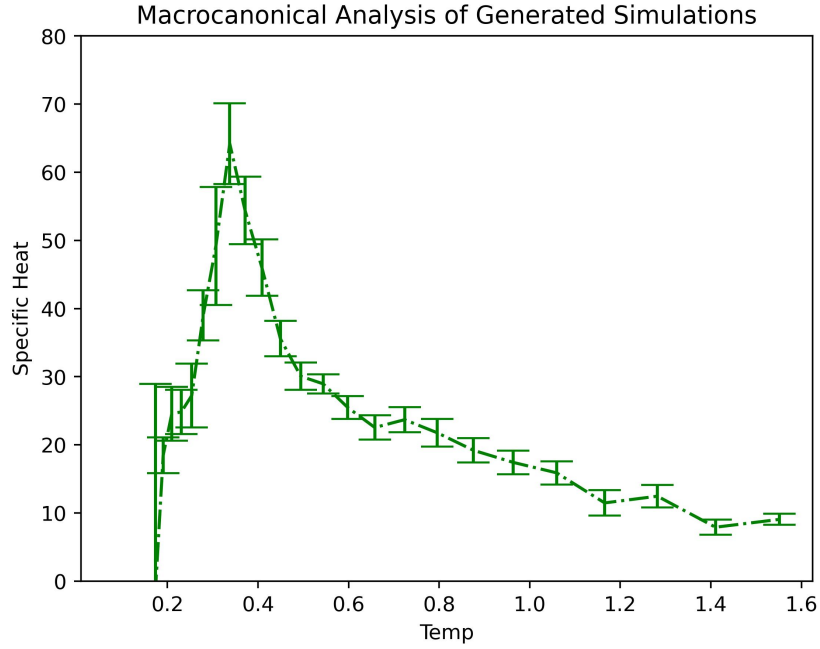


Figure 9: Specific heat v. Temperature plot generated from analysis of post-equilibration data of 26 unique temperature values of the flexible polymer model.

A two-dimensional hyper-phase diagram can be made for the helical polymer model by overlaying multiple specific heat vs. temperature plots for each torsion value and identifying their local maxima. This is shown below in Figure 10.



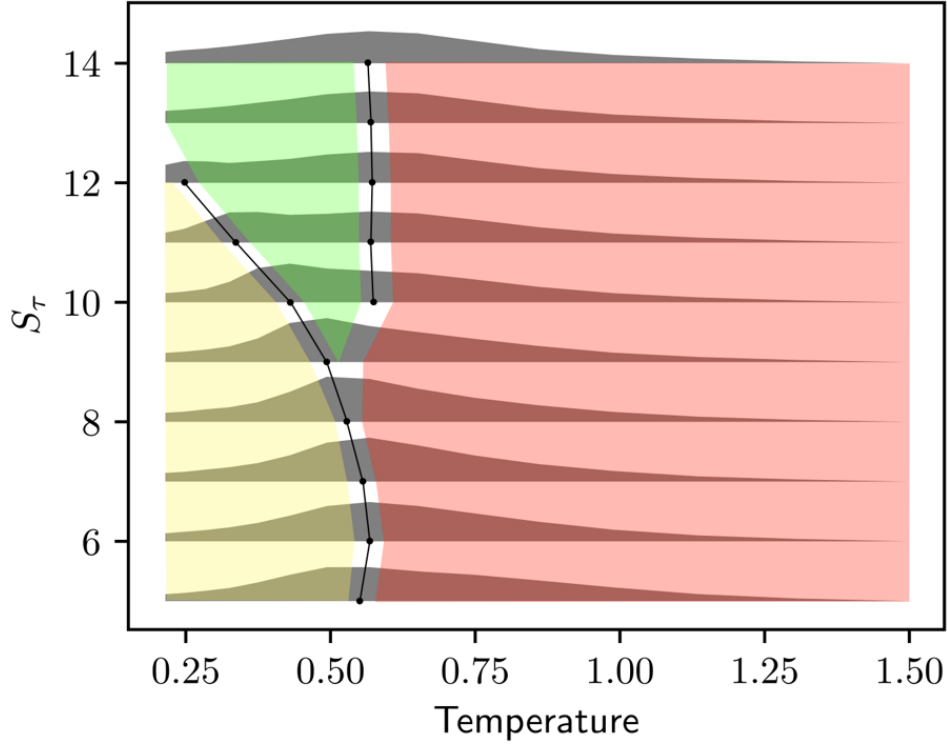


Figure 10: Hyper-phase diagram generated for the helical polymer model across torsion and temperature values. The yellow, green, and red polygons correspond to structures exhibiting helical bundles, a single helix, and random coil-like structures, respectively.

## 5 Conclusions

Flexible and helical homopolymer models, simulated in various programming languages, provide unique insight into the thermodynamics of polymer structures. The generated two-dimensional hyper-phase diagram shows all possible structural phases present in the helical homopolymer model. To obtain this data, equilibration time was analytically determined for each replica. The equilibration time of the 2D parallel tempering exchange scheme decreased by as much as 95% as compared to the 1D simulation shown in Table 1. Efficiency improvements to Monte Carlo simulations, while specifically applied to flexible and helical homopolymer models in this study, allow more simulations at quicker speeds. For the helical model, incorporation of the Hamiltonian exchange into parallel tempering simulations leads to an average of a seven-fold increase in the rate at which new structures are generated. This is most apparent at intermediate torsion strength parameter values representing transitional structures.

While this specific study applied two-dimensional replica exchange to a helical homopolymer model, any Monte Carlo simulation could utilize this across a suitable model parameter. Additionally, it would be interesting to expand my developed program to a two-dimensional Hamiltonian exchange parallel tempering scheme as well as incorporate end-to-end length, a measurable physical dimension, into canonical analysis. Further research steps could involve simulating physical polymers by incorporating the thermodynamic and structural properties of elements into polymer models or exploring additional applications of two-dimensional replica exchange Monte Carlo simulations.

# List of Figures

1	A representation of parallel tempering exchanges is shown for the helical homopolymer model. Threads span a space defined by the torsion parameter, $S_\tau$ , and temperature values. Exchanges between neighboring threads with varied temperatures are shown with black arrows and Hamiltonian exchanges are shown with gray arrows. The orange path is an illustrative example of the random walk performed by a single replica in the two-dimensional parallel tempering approach. . . . .	6
2	A visual representation of the Lennard-Jones and FENE potential values used in both the flexible and helical homopolymer models. . . . .	10
3	A visual representation of the helical homopolymer model generated by Matthew Williams and Michael Bachmann [5]. . . . .	11
4	Depiction of final polymer structure at $T = 0.2$ generated by the developed flexible polymer simulation. Polymer structures from my simulation were plotted using Mathematica code developed by Dr. Williams. . . . .	13
5	Depiction of final polymer structure at $T = 0.7613$ generated by the developed flexible polymer simulation. Polymer structures were plotted using Mathematica code developed by Dr. Williams. . . . .	14
6	Energy of the helical homopolymer model plotted against Monte Carlo time steps. Equilibration time was calculated using the first equilibration algorithm. This specific thread corresponds to a torsion parameter of 10 and a temperature value of 0.303. . . . .	15
7	Energy of a one- and two-dimensional parallel tempering simulation vs. Monte Carlo time step. This data comes from the displacement-only run. For this graph, $S_\tau = 11$ and $T = 0.2$ . Solid lines represent rolling averages with a window size of 250 time-series measurements. $t_{\text{eq}}$ is analytically determined by the stability algorithm and plotted as a vertical dashed line. . . . .	16

8	Average number of time steps per unique configuration measured against the torsion value of the thread for 1-D and 2-D parallel tempering Hamiltonian exchanges for helical homopolymers. The solid points represent the average number of time steps between the appearance of a unique replica structure after energy equilibration at corresponding torsion values shown with sampling errors. (a) corresponds to displacement-only simulations and (b) represents simulations with displacement + global updates. . . . .	18
9	Specific heat v. Temperature plot generated from analysis of post-equilibration data of 26 unique temperature values of the flexible polymer model. . . . .	20
10	Hyper-phase diagram generated for the helical polymer model across torsion and temperature values. The yellow, green, and red polygons correspond to structures exhibiting helical bundles, a single helix, and random coil-like structures, respectively. . . . .	21

## References

- [1] D. Earl and M. Deem, “Parallel tempering: Theory, applications, and new perspectives,” *PHYSICAL CHEMISTRY CHEMICAL PHYSICS*, vol. 7, no. 23, pp. 3910–3916, 2005.
- [2] H. Fukunishi, O. Watanabe, and S. Takada, “On the hamiltonian replica exchange method for efficient sampling of biomolecular systems: Application to protein structure prediction,” *JOURNAL OF CHEMICAL PHYSICS*, vol. 116, pp. 9058–9067, MAY 22 2002.
- [3] Q. Liao, “Enhanced sampling and free energy calculations for protein simulations,” in *COMPUTATIONAL APPROACHES FOR UNDERSTANDING DYNAMICAL SYSTEMS: PROTEIN FOLDING AND ASSEMBLY* (B. Strodel and B. Barz, eds.), vol. 170 of *Progress in Molecular Biology and Translational Science*, pp. 177–213, ACADEMIC PRESS INC ELSEVIER SCIENCE, 2020.
- [4] K. Qi, B. Liewehr, T. Koci, B. Pattanasiri, M. J. Williams, and M. Bachmann, “Influence of bonded interactions on structural phases of flexible polymers,” *JOURNAL OF CHEMICAL PHYSICS*, vol. 150, FEB 7 2019.
- [5] M. J. Williams and M. Bachmann, “Significance of bending restraints for the stability of helical polymer conformations,” *PHYSICAL REVIEW E*, vol. 93, JUN 13 2016.
- [6] M. J. Williams and M. Bachmann, “System-size dependence of helix-bundle formation for generic semiflexible polymers,” *POLYMERS*, vol. 8, JUL 2016.
- [7] D. Sluysmans, N. Willet, J. Thevenot, S. Lecommandoux, and A. Duwez, “Single-molecule mechanical unfolding experiments reveal a critical length for the formation of alpha-helices in peptides,” *NANOSCALE HORIZONS*, vol. 5, no. 4, pp. 671–678, 2020.
- [8] S. A. Sabeur, “First steps toward the construction of a hyperphase diagram that covers different classes of short polymer chains,” *CENTRAL EUROPEAN JOURNAL OF PHYSICS*, vol. 12, pp. 421–426, JUN 2014.
- [9] T. Vogel, J. Gross, and M. Bachmann, “Thermodynamics of the adsorption of flexible polymers on nanowires,” *JOURNAL OF CHEMICAL PHYSICS*, vol. 142, MAR 14 2015.

- [10] B. Liewehr and M. Bachmann, “Smart polymeric recognition of a hexagonal monolayer,” *EPL*, vol. 127, SEP 2019.
- [11] K. Qi, B. Liewehr, T. Koci, B. Pattanasiri, M. J. Williams, and M. Bachmann, “Influence of bonded interactions on structural phases of flexible polymers,” *JOURNAL OF CHEMICAL PHYSICS*, vol. 150, FEB 7 2019.
- [12] P. Liu, B. Kim, R. Friesner, and B. Berne, “Replica exchange with solute tempering: A method for sampling biological systems in explicit water,” *PROCEEDINGS OF THE NATIONAL ACADEMY OF SCIENCES OF THE UNITED STATES OF AMERICA*, vol. 102, pp. 13749–13754, SEP 27 2005.
- [13] S. Zivanovic, F. Colizzi, D. Moreno, A. Hospital, R. Soliva, and M. Orozco, “Exploring the conformational landscape of bioactive small molecules,” *Journal of Chemical Theory and Computation*, vol. 16, pp. 6575–6585, 10 2020.
- [14] J. L. MacCallum, M. I. Muniyat, and K. Gaalswyk, “Online optimization of total acceptance in hamiltonian replica exchange simulations,” *JOURNAL OF PHYSICAL CHEMISTRY B*, vol. 122, pp. 5448–5457, MAY 31 2018.
- [15] I. Y. Akbayrak, S. I. Caglayan, S. Durdagi, L. Kurgan, V. N. Uversky, B. Ulver, H. Dervisoglu, M. Haklidir, O. Hasekioglu, and O. Coskuner-Weber, “Structures of mers-cov macro domain in aqueous solution with dynamics: Impacts of parallel tempering simulation techniques and charmm36m and amber99sb force field parameters,” *PROTEINS-STRUCTURE FUNCTION AND BIOINFORMATICS*, vol. 89, pp. 1289–1299, OCT 2021.
- [16] D. Saha and B. Jana, “Identifying the template for oligomer to fibril conversion for amyloid-beta (1-42) oligomers using hamiltonian replica exchange molecular dynamics,” *CHEMPHYSCHEM*, vol. 23, DEC 16 2022.
- [17] H. Katzgraber, S. Trebst, D. Huse, and M. Troyer, “Feedback-optimized parallel tempering monte carlo,” *JOURNAL OF STATISTICAL MECHANICS-THEORY AND EXPERIMENT*, MAR 2006.

- [18] D. Gront and A. Kolinski, “Efficient scheme for optimization of parallel tempering monte carlo method,” *JOURNAL OF PHYSICS-CONDENSED MATTER*, vol. 19, JAN 24 2007.
- [19] M. Athenes and F. Calvo, “Multiple-replica exchange with information retrieval,” *CHEMPHYSCHEM*, vol. 9, pp. 2332–2339, NOV 10 2008.
- [20] M. K. Prakash, A. Barducci, and M. Parrinello, “Replica temperatures for uniform exchange and efficient roundtrip times in explicit solvent parallel tempering simulations,” *JOURNAL OF CHEMICAL THEORY AND COMPUTATION*, vol. 7, pp. 2025–2027, JUL 2011.
- [21] A. Malakis and T. Papakonstantinou, “Comparative study of selected parallel tempering methods,” *PHYSICAL REVIEW E*, vol. 88, JUL 30 2013.
- [22] B. Yucesoy, J. Machta, and H. G. Katzgraber, “Correlations between the dynamics of parallel tempering and the free-energy landscape in spin glasses,” *PHYSICAL REVIEW E*, vol. 87, JAN 4 2013.
- [23] S. Schnabel, D. T. Seaton, D. P. Landau, and M. Bachmann, “Microcanonical entropy inflection points: Key to systematic understanding of transitions in finite systems,” *PHYSICAL REVIEW E*, vol. 84, JUL 18 2011.
- [24] K. Qi and M. Bachmann, “Classification of phase transitions by microcanonical inflection-point analysis,” *PHYSICAL REVIEW LETTERS*, vol. 120, APR 30 2018.
- [25] M. Rubinstein, *Polymer physics / Michael Rubinstein and Ralph H. Colby*. Oxford ;: Oxford University Press, 2007.
- [26] J. Moreno, H. Katzgraber, and A. Hartmann, “Finding low-temperature states with parallel tempering, simulated annealing and simple monte carlo,” *INTERNATIONAL JOURNAL OF MODERN PHYSICS C*, vol. 14, pp. 285–302, MAR 2003.
- [27] A. Fischer and C. Igel, “A bound for the convergence rate of parallel tempering for sampling restricted boltzmann machines,” *THEORETICAL COMPUTER SCIENCE*, vol. 598, pp. 102–117, SEP 20 2015.
- [28] N. Giordano and H. Nakanishi, *Computational Physics*. Pearson/Prentice Hall, 2006.

- [29] N. Metropolis and S. Ulam, “The monte carlo method,” *Journal of the American statistical association*, vol. 44, no. 247, pp. 335–341, 1949.
- [30] H. S. Hsich, “Dynamics of polymeric liquids, second edition volume 2: Kinetic theory, r. byron bird, charles f. curtiss, robert c. armstrong, and ole hassager, wiley-interscience, new york, 1987, 437 pp. price: \$65.00.,” *Journal of Polymer Science Part C: Polymer Letters*, vol. 25, no. 12, pp. 511–511, 1987.
- [31] K. Kremer and G. S. Grest, “Dynamics of entangled linear polymer melts: a molecular-dynamics simulation,” *The Journal of Chemical Physics*, vol. 92, no. 8, pp. 5057–5086, 1990.
- [32] J. Llibre and Y. Long, “Periodic solutions for the generalized anisotropic lennard-jones hamiltonian,” *QUALITATIVE THEORY OF DYNAMICAL SYSTEMS*, vol. 14, pp. 291–311, OCT 2015.